

# Ion transport from the source to first cyclotron orbit

Jean-Loup Belmont

**Abstract** The ions produced by an external source and axially injected into the cyclotron are considered. The ion beam, with a matching structure, must be carefully placed on the orbit to be accelerated and well extracted. One has to take into account its position on the first turn, its shape, its chopped time structure due to RF (radio-frequency). A compromise between different necessities must be obtained. In fact beam losses can be significant, and the ion transfer efficiency from the source to the orbit varies from a few per cent to 70%!

**Key words** axial injection • cyclotron

## Introduction

About 40 compact cyclotrons (AVF) are inventoried inside the “Proceeding of the 16th International Conference on Cyclotrons and their Applications 2001” and about 75% are equipped with a system of low energy injection of ions. Research laboratories have equipped their AVF cyclotrons with such “axial injections” because they need very stable beams and various ions which require external sources. For that purpose, the beam is delivered from the source to the cyclotron; it has to pass through the magnet yoke by a narrow vertical channel, then an electrostatic inflector bends its direction by 90 degrees towards the first accelerated orbit located inside the horizontal median plane.

The design depends on the flexibility of the machine to be matched to accommodate different mechanical devices; it depends also on available space, on the desired quality and efficiency, on the money, on manpower (and its qualification) that the laboratory can afford [5–8, 29].

## The low energy beam transport line

The ions are extracted from the source, analysed, the desired beam is formed, and emittance calibrated – Fig. 1. The transfer line may be from 1 or 2 m long, or even about 40 m if ion source is out of the cyclotron cave. A line several meters long has to be used to match carefully the beam to the internal orbit, with corrections for chromatism, isochronism, stigmatism [24, 26]. Very long lines are now studied or are under construction with cascade of machines for radioactive ion beams [2, 23]; then a part of the line is only devoted to the simplest possible transport. For each part, an appropriate method of calculation is chosen, taking into account the technology of fabrication, space available,

J.-L. Belmont  
Institut des Sciences Nucléaires,  
53 des Martyrs Ave., F 38026 Grenoble-CEDEX, France,  
e-mail: jean-loup.belmont@wanadoo.fr

Received: 26 November 2002, Accepted: 10 April 2003

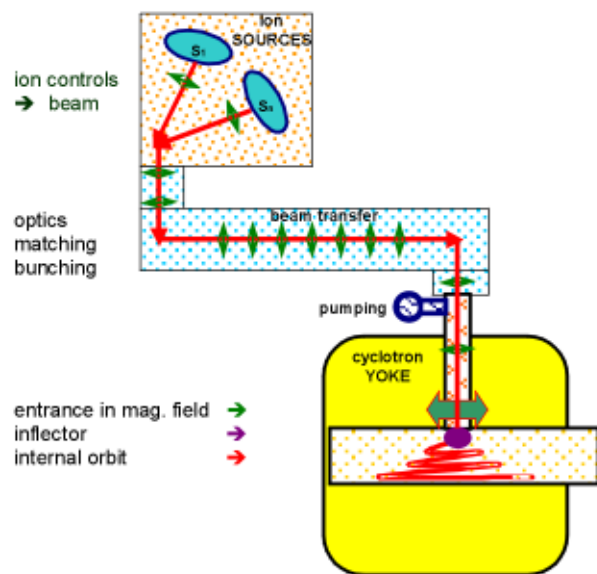


**Fig. 1.** Diagram of axial injection.

time devoted for the studies, construction, and price. This latter consideration has often been important. Inside the cyclotron yoke one pays special attention to the quality of the vacuum, the magnetic stray fields, the “matching” of the emittances, the reliability of the elements [19, 25]. The optics is made of magnets, deflectors, and lenses, see Tables 1 and 2.

**Table 1.** Cylindrical lenses.

Cylindrical	Einzel	Glaser
Advantages stigmatic	low price compact	quality shielded
Drawback for low energy	aberrations sparking	large expensive axis rotation
Users	must be well centered used at source exits (Ganil, ...)	for beam line Berkeley, Catania (12), China, JAERI, Jülich, Jyväskylä, MSU, South Africa, ... inside yoke

**Table 2.** Quadrupole lenses.

Quadrupole	Electrostatic	Magnetic
Advantages astigmatic	low cost	good vacuum efficient at high energy
Drawback astigmatic bulky, long disturbed by stray field	outgazing	high cost
Users	Vancouver (77) k500 – MSU Texas, Agor, ...	GANIL-Louvain, JINR-Dubna, for matching

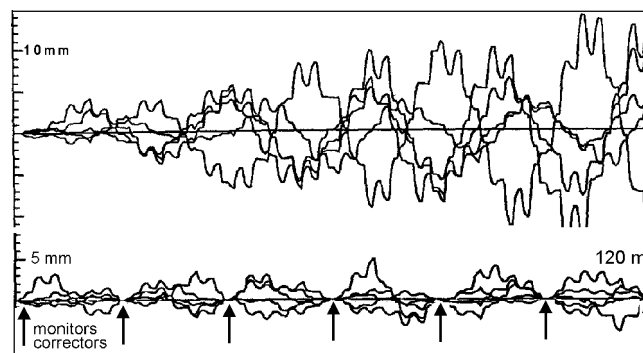


**Fig. 2.** Central trajectories around a theoretical straight axis for 5 different sets of positioning errors of lenses, stochastically distributed,  $\sigma = 0.3$  mm and 0.1 mrad.

### Centering of optics

It takes a little to perturb a beam of low energy: one needs diagnostics and correcting devices. There are positioning errors in the alignment of optical elements, and diagnostic elements are also misaligned. External stray fields can perturb the ideal trajectory. With correctors and monitors the machine operators must minimize these effects.

For example, at Grenoble [17, 23] we have studied a 120 m long line; it was a periodic focusing structure FODO, provided with magnetic quadrupoles without iron. We have experimented on such a 18 m long line only. Figure 2 shows 5 positions of the central trajectory along a theoretical axis, obtained with 5 different sets of positioning errors of optical elements which are stochastically distributed (Gaussian distribution with  $\sigma = 0.3$  mm and 0.1 mrad) and the effect of corrections each 18 m. Figure 3 shows the influence of earth magnetic field. Stronger is the focusing of a lens, the off centre moving is larger; so the betatron oscillation by pattern must be rather small, like the number of lenses, otherwise one must increase the number of correctors.

### Space charge effects

Equations of Lapostole or Sacherer [30] describe the evolution of the beam envelope with space charge effects which are included in the code “Transport” (CERN, PSI, others). They are easy to use, but sometimes they do not describe exactly the reality because of capture of electrons and do not include the increase of the emittance along the path. For a pulsed beam, ellipsoid or spherical models of charge distribution are used [10]. An example: let us assume a small current of  $\text{Ar}^{6+}$  accelerated by  $V = 10$  kV,

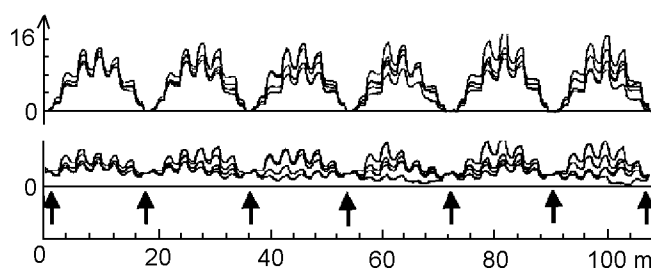


**Fig. 3.** Like Fig. 2, but with effects of corrections in the presence of earth magnetic field, and corrected by an out centering.

$\pi\epsilon = 80\pi$  mm-mrad, focused by lens with the average focus per meter  $f = 1.7$  m, for keeping the same beam diameter with  $10 \mu\text{A}$  one finds that the focus must decrease to 1.35 m. We understand that optics must be adjusted with pulsed beams at full intensity. To decrease the space charge effects, a solution is to increase the focusing per meter. A better solution is to increase the ion source high voltage  $V$ : the emittance decreases like  $V^{-1/2}$  and the limiting current like  $V^{3/2}$ . Other advantages, with a higher energy the beam is less perturbed by external magnetic fields and the focusing of the beam during the first turns inside the machine is less dependent on the RF phase. Inconveniences include, design, cost, sparks, difficult use of cylindrical lenses, power consumption of optics, higher voltage of RF applied to the dee for clearing the centre. At several hundred kilovolts, like at PSI [34], the problems are different than those exposed here, but the quality of the beam of this machine shows that it is a very good solution!

### Vacuum effects

The design of the beam line must include the requested level of the vacuum. For an ion of charge  $q$ , the transmission  $T$ , through a tube  $L$  meter long, with a known residual gas at the pressure  $P$ , is  $T = e^{-(C\sigma LP)}$ . The cross section of the charge exchange in the gas target is  $\sigma$  ( $\sigma$  is given with a good approximation by A. Schlachter [33]).

At Grenoble, the transmission  $T$  has been measured on the 18 m long test bench. We found that practically  $\sigma$  is independent of the energy. The transmissions  $T$  of the  $\text{Rb}^{1+}$ , depending on gas, with  $P$  in mbar, are:

$$\begin{aligned} \text{nitrogen: } T &= e^{-19100.P}; \text{ argon: } T = e^{-20060.P}; \\ \text{xenon: } T &= e^{-38700.P}; \text{ helium: } T = e^{-2390.P}. \end{aligned}$$

Our measured  $\sigma$  [23] are 2 times smaller than these from Schlachter's equation.

At the pressure where the charge exchange is small, the increase of the emittance is negligible. For example, for  $\text{Rb}^{1+}$  inside nitrogen at pressure  $2 \times 10^{-5}$  mbar, the emittance increase is  $9\pi$  mm-mrad (measured and calculated), but it is zero at  $10^{-6}$  mbar. About losses of  $\text{H}^-$ , see Ref. [18].

### The accelerated equilibrium orbit

The beam must reach the central plane of the machine on the equilibrium orbit.

### To find the position of the first orbit and its beam shape

Central region designs for various accelerating systems have been described extensively [5, 7, 13, 19, 20, 22, 27, 31, 35]. The ways for obtaining these orbits are miscellaneous, from the simplest to the most sophisticated code of the integration of the movements due to fields, themselves either measured or calculated with codes. The general process is:

1. To find a stable central orbit and its eigen emittance for the central RF phase of the burst accelerated, a little far from the centre.
2. To calculate (or estimate!) the backward trajectory through the dee tips up to the first dee-dummy dee gap.

At that point one seeks how is the actual beam which can be realised and injected in fact, then one calculates forward this set of particles and one verifies that it is well accelerated [14, 24].

3. To define a real inflector satisfying to the preceding conditions.
4. To calculate the injected beam upon the hole yoke axis: (see Fig. 4, axis at the point O, with its centre of curvature  $\Omega$  and radius of curvature  $Rm$ , the inflector exit at the point S). Throughout the inflector, the axial injection should provide the relevant beam like it has been previously calculated. This emittance depends on the RF phase too: a perfect matching to a large phase range is impossible.
5. To do a lot of iterations for adapting the designs, specially the design of dee tips and eventually of the inflector.
6. To find the technical structures for each RF harmonic, mainly the shapes of dee tips and of the deflectors. These devices must not interfere. The beam path is normally operated in constant orbit mode, i.e. all ions follow the same trajectory independently of their charge, mass and of the magnetic field level, for a given harmonic mode.

### Some ideas helping to find the geometry of the centre

It is time consuming to calculate the fields with sufficient accuracy and to compute the movements due to the forces. Many changes are proposed, so it is interesting to foresee qualitatively what the change will do. If an accelerating interval of length  $d$  has an electric field  $E$  of the form:  $E = E_0 \sin\varphi$  with  $E_0$  constant and  $\varphi = (\omega t + \varphi_0)$  (hard edge approximation inside  $d$ ), the equation of motion can be integrated analytically to yield a simple relationship between the initial values  $R_0, \alpha, \varphi_0$  and the final ones  $R_s, \beta, \varphi_s$  (Fig. 5). One finds that the centre of curvature has been displaced perpendicularly to electric field direction ( $E_0$ ) by: [7, 20].

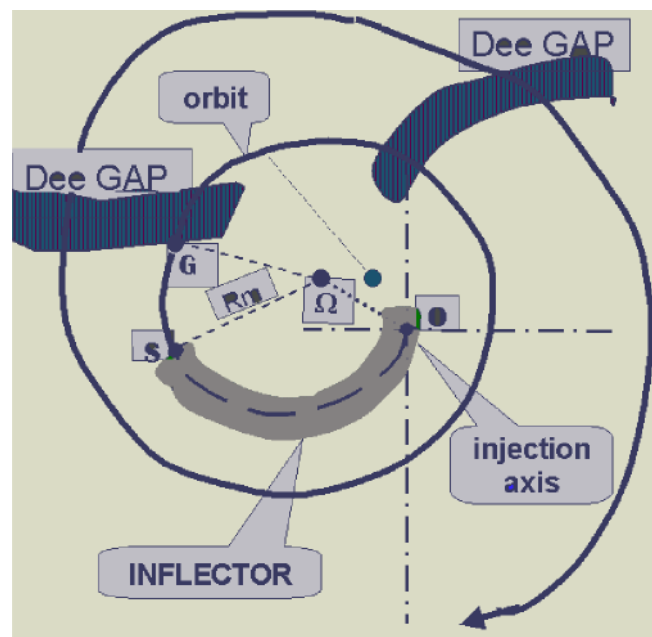


**Fig. 4.** Diagram of the trajectory centering.  $\Omega$  is the curvature centre at the inflector exit.

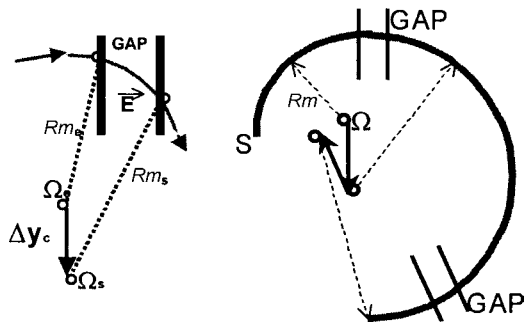


**Fig. 5.** Roughly, the cyclotron symmetry axis is close to the middle of the oscillation centres: one has  $\Delta y_c/2 < Rm$ . If the hole inside the yoke is along this axis, the mirror or spiral inflector is used ( $\Omega < Rm$ ).

$$(1) \quad \Delta Y_c = (R_0/2dh) \{ \sin(\Delta\phi + \phi_0) - \sin\phi_0 \}$$

with  $\Delta\phi = h\omega_{ion} \Delta t_s$

where:  $h$  = RF harmonic vs. ions. Generally,  $h$  is not integer here (bump or well of magnetic field). For simple, precise and fast calculation, each dee gap can be decomposed into 10 to 20 gaps by equipotential parabolas. Each gap can be moved independently in one piece, very fast (by a code), and the shape of the dee tips easily found as shown in Fig. 6. Close to the centre, the magnetic focusing is not significant but the focalisation is created by the accelerating gaps. The presence of posts (rods crossing the median plane) or not, changes the focalisation which is RF phase dependent. Roughly, without vertical post the vertical focusing is twice more efficient and during the gap crossing the phase shift is larger, the horizontal focalisation is zero. Beam centring is easier with several posts, but the number of those posts is limited, indeed it is difficult to include many orbits – one for each RF harmonics with their different posts – inside such a close space. The complexity of the matching is due to the coupling between the phase spaces at different locations, from the source to the internal accelerated beam.

**Inflectors**

The calculations indicate where to inject the beam. There are three types of inflector for bending the beam direction by an angle of 90° to the good orbit [32].

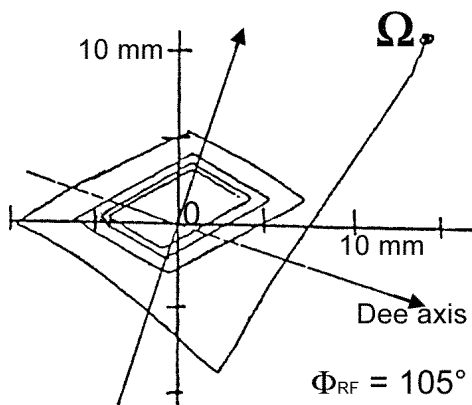


**Fig. 6.** An example of centres of rotation after the inflector exit. ( $\Omega$ ): loci of rotation axis during the first turns in the Grenoble cyclotron, (2 dees, 4 gaps).

**The electrostatic mirror**

An electrostatic field is applied between 2 planar electrodes which are positioned at an angle of about 45 degrees to the incoming ion beam. It produces the bend required with a little rotation in addition [6, 7, 11, 16, 29, 32]. The electrostatic mirror is attractive from the standpoint of simplicity and its reduced volume; it is not limited to work at “constant orbit” unlike the 2 other types of inflectors. It has the disadvantage that the applied potentials must be of the same order of magnitude as the ion source potential; the great currents of heavy ions destroy its grid which has to be periodically changed. At its exit the choice of the position of the centre of curvature is poor. Its use is mainly reserved for a cyclotron with only one active dee like at Berkeley and at the compact cyclotron of PSI. Its focusing and the coupling produced by its transfer matrix are both weak. Inside the superconducting cyclotrons, first proposed, this inflector has been abandoned for spiral type (Agor, Catania, MSU).

**The spiral inflector (or Belmont–Pabot inflector)**

It should be a cylindrical deflector in absence of a magnetic field, but in presence of the axial magnetic field  $B_z$ , the vertical plane rotates as the particles gain radial velocity. Figure 7 shows the projection of the ion trajectory on the median plane of the cyclotron as a function of the par-

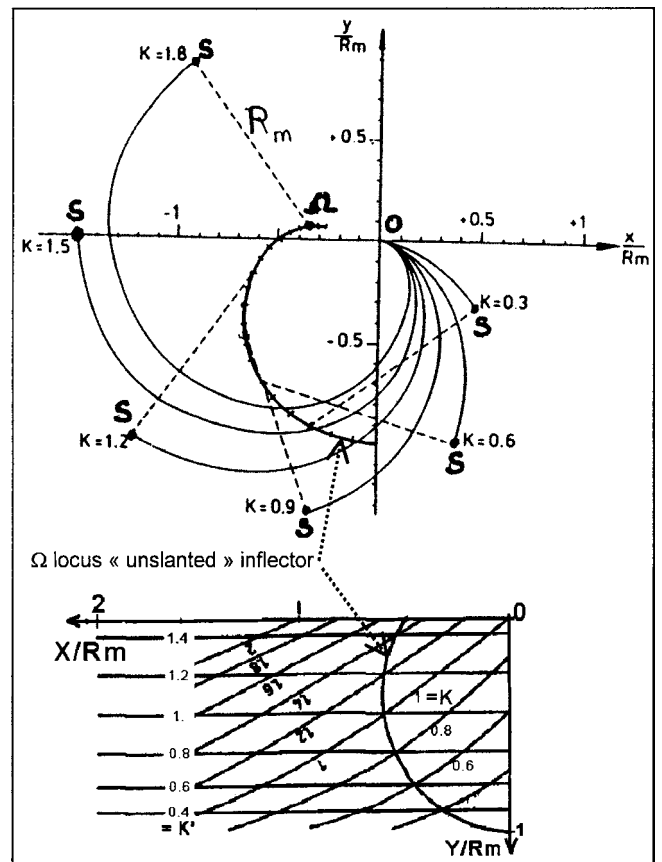


**Fig. 7.** Spiral inflectors: projections in median plan of trajectories (unslanted inflectors) and of curvature centres at its exit, for unslanted and slanted designs.

ameter  $K_0$  and the locus of the corresponding orbit centre of curvature (point  $\Omega$ ) at the exit. ( $A$  = electrical radius of curvature,  $Rm$  = magnetic radius of curvature and  $K_0 = A/2Rm$ .) Its height is  $A$ . The distance  $O\Omega$  is always smaller than  $Rm$  or  $O\Omega \ll Rm$  (compactness).

To obtain a more flexible design, a radial electric field component, proportional to the magnetic force along the trajectory can be introduced. It is "a spiral inflector with slanted electrodes". That way, a more adjustable shift of the orbit centre at the exit can be obtained. Inside these spiral deflectors, the differential equations of the trajectories [7, 28] are very coupled and must be numerically integrated. The obtained transfer matrix is very coupled [1] and indicates an apparent emittance increase due to its observed projections in  $X, X'$  and  $Y, Y'$  planes. It is the price of its compactness.

### The hyperboloid inflector

The electrodes are formed by two pieces of concentric hyperboloids (Fig. 8). As the beam goes along close to median plane, the electric field contributes less to bend it. So the inflector is not compact. There are no free par-

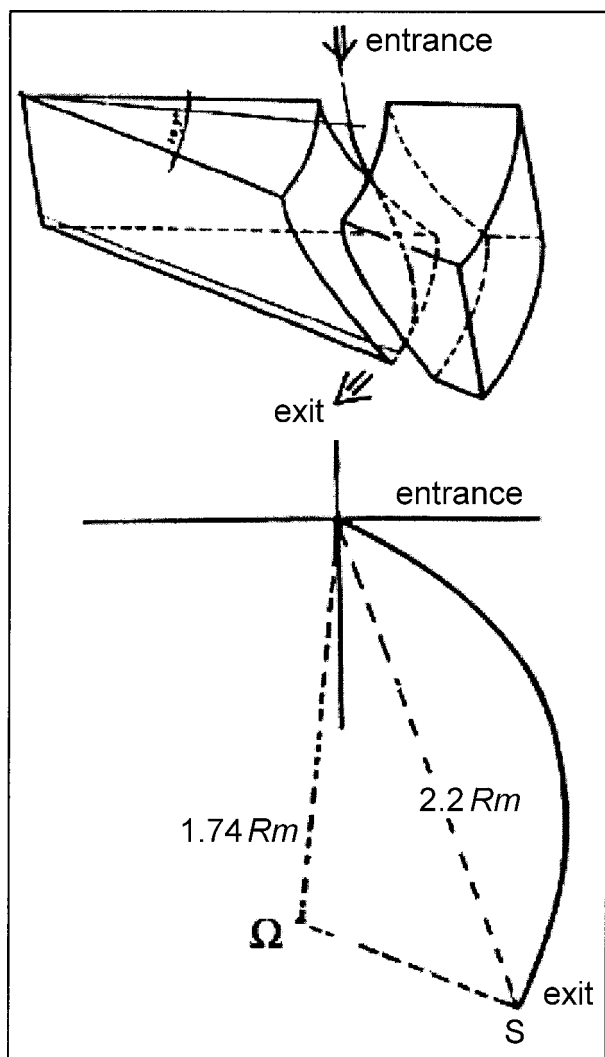


Fig. 8. Hyperboloid inflector: projections in median plan of trajectories and curvature centre at its exit.

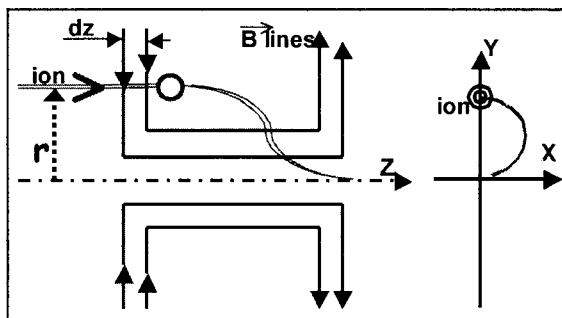


Fig. 9. Movement of ions inside a magnetic lens: longitudinal effects and transversal projections, hard edge model,  $B = \text{constant}$ .

ameters for the choice of the centre of rotation  $\Omega$ . The distance between  $\Omega$  and the injection axis is  $1.74Rm$  and this axis is different from the axis of symmetry of the cyclotron: the hole inside the yoke is at that position, which is conceivable only without magnetic saturation.

The differential equations of trajectories inside this inflector are analytically solved; the transfer matrix is given by analytic calculation. The main advantage is that this matrix is decoupled (for a particular choice of the axes of Reference), therefore the hyperbolic inflector allows computing optics of a good quality [11]. It is used inside Julic, Ganil cyclotrons. Inconvenient is its dimensions and the only low beam energy that it accepts.

### Focusing of the cylindrically symmetric magnetic lenses

A coupling of the motion is given by the magnetic field inside the yoke, along the beam injection. In the magnetic Glaser lenses the beam arrives from a part without field, (hard edge model, Fig. 9) and, when it enters inside the field, it crosses the magnetic lines which have a radial component  $B_r$ , proportional to the radius, which gives the ions a transversal velocity leading them to motion of rotation (Larmor rotation) and a focusing effect (diameter =  $r$ ). The rotation stops with the field. That way, the beam must be injected centred on the axis of symmetry of the magnetic field, and it arrives inside the inflector with that velocity of rotation (which continues in fact inside the inflector). Due to the effects of iron saturation, the shape of the field depends on the used magnetic field level, the beam is not a "constant orbit" – like supposed in all calculations involved – the focalisation changes and must be adjusted. An other effect of the stray field is that the lengths of the paths are different along the axis and at the radius  $r$  (Fig. 9): the lens is not isochronous [4].

### Emittance matching

An accelerated uncoupled beam, calculated backward through the (spiral) inflector is coupled [12]:

1. We try to obtain that coupling by forward computation of the transport line and it is a long way to do so! See CIME at Ganil: time of calculation and available space for optics [3, 24].
2. More generally the matching is only satisfied with an approximate superposition of the emittance projections in the used coordinates  $xx', yy'$ , emittances obtained

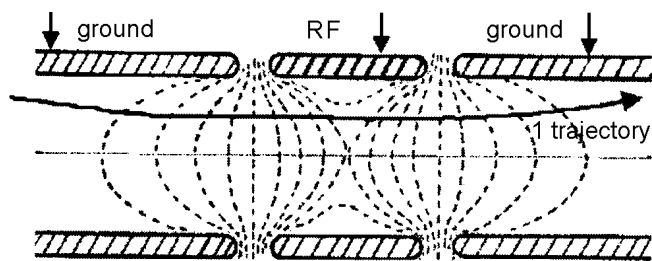


Fig. 10. Tube for bunching application (without grid).

- backward from the cyclotron internal orbit and forward from the transport line (for example calculated at the inflector exit or at the entrance inside yoke stray field).
3. The beam diameter must pass throughout all injection devices.

### Bunching

By modulating of the velocity of the continuous beam more particles can be squeezed inside the RF phase range of acceleration. The idea is: 1) upstream above the inflector, to decelerate particles in advance relatively to a central particle and to accelerate the late particles; 2) the ions join together inside a narrow range of RF phase if a linear velocity variation is applied; 3) the farther from the inflector this bunching is applied, the smaller acceleration–deceleration is to be applied, but it is more sensitive to perturbations; 4) It is more difficult to realize a linear (sawtooth) variation of the velocity than to use sine variations.

#### Sine bunching

Several axial injection systems employ a simple sine wave RF modulation (intensity gain: 3 to 5 – without space charge effects). The buncher is a tube, (a micro linear accelerator) on which several hundred volts RF are applied (Fig. 10). Naturally, the RF phase has to be adjusted to the internal accelerated burst.

#### Sawtooth bunching

To go closer towards a linearly velocity variation, RF harmonics are used (Fig. 11), with tubes there are easily applied [21, 36]. The obtained intensity gain is 8 to 15 – without space charge. An interesting solution is the use of a single gap with a double grid [15] and to apply a tension close to a sawtooth (Fig. 12), but with the inconvenience of grids and fast electronics. It uses a tube but with so large first

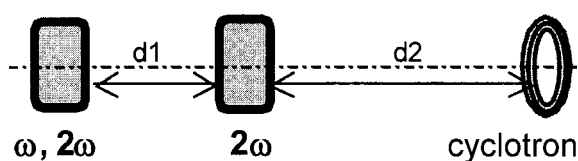


Fig. 11. Several tubes apply the different harmonics, but a distance between tubes is equivalent to more harmonics. (Here, VEEC of India proposition.)

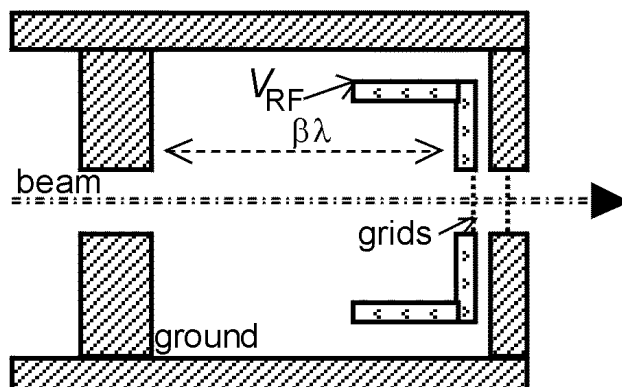


Fig. 12. The RF voltage is applied on internal electrode, the external one is grounded. The RF accelerating field is in between the 2 gridded electrodes. The integral of the effect of the left field is zero.

gap at its entrance that integrated energy gain is zero (first  $\beta\lambda$  gap width) and, in contrary, a terminal narrow gridded gap gives an energy gain closed to  $q V_{RF}(t)$ , where  $V_{RF}(t)$  is the voltage applied on the electrode.

#### Perturbations of the bunching

The energy spread is the main cause of perturbations; it comes from the power supply (roughly  $1^\circ\text{RF}/\text{V}$ ), the “inflating” of the crossed equipotentials of the buncher (Fig. 10), and from the space charge. We have seen another cause: the trajectories along the yoke with saturated iron have not the same length [4]. At the bunching itself it corresponds to an energy spread which perturbs the non-chromatic optics.

#### Cures of perturbations

The “inflating” of the equipotentials is compacted in the small tube, slightly gridded. A positioning of the buncher close to the inflector cures the space charge, but this imposes a high variation of the velocity which disperses the beam at the inflector exit. For the highest intensities, the bunching, ineffective, is not used.

#### Codes

A number of very confident codes are written, and available (unhappily not always very well exportable!). Note: LIONS (orbits), GALOPR and SOSO (space charge, bunching, trajectory), CHA3D (map) at Ganil/Caen [9]; and RELAX3D (maps), CASINO (inflector), SPUNCH (bunching) at Triumf/Vancouver, TRANSPORT (beam), POISCR (map) at CERN, etc.

#### Conclusion

The choice of devices results from compromises taking into account: the feasible implementations on the actual machine, the accuracy of the known charts of fields in one’s pos-

session, the time assigned to the task. These choices will depend upon the different means of the laboratory: financial, calculation, conception and realizations. To build an axial injection is always a challenge. Now, one can have the help of broad studies which have been done on the subject all over the world. Roughly, if the number of dees is the same, the centres are not very different or are homothetic: then this can help to start a project. The adaptation of the beam to the cyclotron centres is a difficult part. Nevertheless, whatever the relentlessness to find solutions, generally one cannot solve all the problems for all RF harmonics: the cyclotron users have to choose the main range of energy and to limit the diversity of the particles to be accelerated.

Depending on the designs, the ion transfer efficiencies, from the head of the beam transfer to the internal orbit, varies from a few per cent up to 70%. Common values are rather 10% to 20%.

**Acknowledgments** The author would like to acknowledge the help of people who supplied information for this paper.

## References

- Balden RJ, Kleeven W, Milinkovic LS *et al.* (1989) Aspect of phase space. In: Proc of the 12th Int Conf on Cyclotrons and their Applications, 8–12 May 1989, Berlin, Germany. World Scientific, Singapore, pp 435–438
- Bashevoy VV, El Shazly MN, Gulbekian GG *et al.* (2001) Simulation of the transmission efficiency of the Dribs transport lines. In: Proc of the 16th Int Conf on Cyclotrons and their Applications held at NSCL/MSU, 13–17 May 2001, East Lansing, USA. AIP 600:387–390
- Beck AR, Chel S, Bru B (1989) 6-dimensional beam matching for axial injection. In: Proc of the 12th Int Conf on Cyclotrons and their Applications, 8–12 May 1989, Berlin, Germany. World Scientific, Singapore, pp 432–435
- Bellomo G (1986) The Axial injection project for the Milan superconducting cyclotron. In: Proc of the 11th Int Conf on Cyclotrons and their Applications, 13–17 October 1986, Tokyo, Japan. Ionics Publishing, Tokyo, pp 503–506
- Bellomo G (1989) The central region for compact cyclotrons. In: Proc of the 12th Int Conf on Cyclotrons and their Applications, 8–12 May 1989, Berlin, Germany. World Scientific, Singapore, pp 325–334
- Bellomo G, Johnson D, Marti F (1983) On the feasibility of axial injection in superconducting cyclotrons. Nucl Instrum Meth Phys Res 206:19–46
- Belmont J-L (1986) Axial injection and central region of AVF cyclotrons. In: Lecture notes of 1986 RCNP KIKUCHI Summer School on Accelerator Technology. Osaka, Research Center for Nuclear Physics, Osaka, pp 79–124
- Belmont J-L (2002) Ion transport. Int. Report ISN-02-47. Institut des Sciences Nucléaires, Grenoble
- Bertrand P, Bibet D, Bourgarel MP *et al.* (1988) SPIRAL facility at Ganil: ion beam simulation and optimisation method for the CIME cyclotron injection system. In: Baron E, Lieuvain M (eds) Proc of the 15th Int Conf on Cyclotrons and their Applications, 14–19 June 1998, Caen, France. IOP, Bristol, pp 458–461
- Bertrand P, Ricaud C (2001) Specific cyclotron correlations under space charge effects in the case of spherical beam. In: Proc of the 16th Int Conf on Cyclotrons and their Applications held at NSCL/MSU, 13–17 May 2001, East Lansing, USA. AIP 16:379–382
- Botman JIM (1989) Axial deflectors and the correlation between phase spaces. In: Proc of the 12th Int Conf on Cyclotrons and their Applications, 8–12 May 1989, Berlin, Germany. World Scientific, Singapore, pp 443–446
- Botman JIM, Hagedoorn HL, Reich J (1988) The beam emittance of cyclotrons with an axial injection system. In: Tazzari S (ed.) Proc of the 1st European Particle Accelerator Conf: EPAC-1, 7–11 June 1988, Rome, Italy. Vols 1–2. World Scientific, Singapore, pp 651–653
- Bourgarel MP, Baron E, Attal P (1989) Modification of the Ganil injection. In: Proc of the 12th Int Conf on Cyclotrons and their Applications, 8–12 May 1989, Berlin, Germany. World Scientific, Singapore, pp 111–115
- Bourgarel MP and SPIRAL/GANIL groups (1998) SPIRAL facility: first results on the CIME Cyclotron. In: Baron E, Lieuvain M (eds) Proc of the 15th Int Conf on Cyclotrons and their Applications, 14–19 June 1998, Caen, France. IOP, Bristol, pp 311–318
- Chabert A, Ricaud C, Boy L *et al.* (1999) The linear buncher of SPIRAL. Nucl Instrum Meth Phys Res A 423:7–15
- Clark DJ, Lyneis CM (1986) Berkeley 88-inch cyclotron. In: Proc of the 11th Int Conf on Cyclotrons and their Applications, 13–17 October 1986, Tokyo, Japan. Ionics Publishing, Tokyo, pp 499–502
- De Conto JM (1994) Radioactive ion beams at Grenoble: beam transport and acceleration. In: Proc of the 4th European Particle Accelerator Conf, 27 June – 1 July 1994, London, UK. World Scientific, Singapore, pp 560–562
- Heikkinen P, Liukkonen E, Niemirrn P *et al.* (1998) Feasibility studies of H<sup>-</sup> acceleration. In: Baron E, Lieuvain M (eds) Proc of the 15th Int Conf on Cyclotrons and their Applications, 14–19 June 1998, Caen, France. IOP, Bristol, pp 650–653
- Heikkinen P, Rinta-Nikkola M (1992) Ion optics in the Jyväskylä K130 cyclotron. In: Proc of the 13th Int Conf on Cyclotrons and their Applications, 6–10 July 1992, Vancouver, Canada. World Scientific, Singapore, pp 392–395
- Khallouf A (1986) Trajectoires centrales. Ph.D. Thesis. Grenoble University
- Linch FJ, Lewis RN, Bollinger LM *et al.* (1979) Beam buncher for heavy ions. Nucl Instrum Meth Phys Res 159:245–263
- Marti F, Cavalya A (1986) Axial injection in the K500 superconducting cyclotron. In: Proc of the 11th Int Conf on Cyclotrons and their Applications, 13–17 October 1986, Tokyo, Japan. Ionics Publishing, Tokyo, pp 484–487
- Nibart V (1996) Transport d'ions exotiques de basse energie sur longue distance. D.Sc. Thesis, Grenoble University. Int. Report ISN-96-01. Institut des Sciences Nucléaires, Grenoble
- Ricaud C, Attal P, Baron E *et al.* (1989) Preliminary design of a new high intensity injection. In: Proc of the 12th Int Conf on Cyclotrons and their Applications, 8–12 May 1989, Berlin, Germany. World Scientific, Singapore, pp 372–375
- Ricaud C, Attal P, Baron E *et al.* (1990) Status of the new high intensity injection system. In: Proc of the 2nd European Particle Accelerator Conf, 12–16 June 1990, Nice, France. Editions Frontières, Gif-sur-Yvette, pp 1252–1254
- Ricaud C, Baron E, Bony J *et al.* (1992) Commissioning of the new high intensity axial injection for GANIL. In: Proc of the 13th Int Conf on Cyclotrons and their Applications, 6–10 July 1992, Vancouver, Canada. World Scientific, Singapore, pp 446–449
- Rifuggiato D, Calabretta L, Shchepunov VA *et al.* (1998) Axial injection in the LNS superconducting cyclotron. In: Baron E, Lieuvain M (eds) Proc of the 15th Int Conf on Cyclotrons and their Applications, 14–19 June 1998, Caen, France. IOP, Bristol, pp 646–649
- Root L (1972) Design of an inflector for Triumf cyclotron. Ph.D. Thesis. University of British Columbia, Vancouver
- Ryckewaert GH (1981) Axial injection systems for cyclotrons. In: Proc of the 9th Int Conf on Cyclotrons and their

- Applications, 7–10 September 1981, Caen, France. Les Editions de Physique, Les Ulis, pp 241–247
30. Sacherer FJ (1971) RMS envelope equations with space charge. *IEEE Trans Nucl Sci NS* 18:1105–1107
  31. Schapira JP, Le Goff A, Brizzi R (1989) Agor central region design. In: Proc of the 12th Int Conf on Cyclotrons and their Applications, 8–12 May 1989, Berlin, Germany. World Scientific, Singapore, pp 335–338
  32. Schapira JP, Mandrion P (1984) Axial injection in the Orsay Project of a superconducting cyclotron. In: Proc of the 10th Int Conf on Cyclotrons and their Applications, 30 April – 3 March 1984, East Lansing, USA. IEEE Press, New York, pp 332–336
  33. Schlachter AS (1984) Charge changing collisions. In: Proc of the 10th Int Conf on Cyclotrons and their Applications, 30 April – 3 March 1984, East Lansing, USA. IEEE Press, New York, pp 563–570
  34. Schryber U, Adam S, Berkes B *et al.* (1981) Status report on the new injector at SIN. In: Proc of the 9th Int Conf on Cyclotrons and their Applications, 7 – 10 September 1981, Caen, France. Les Editions de Physique, Les Ulis, pp 43–46
  35. Toprek D, Goto A, Yano Y (1999) Beam orbit simulation in the central region of the RIKEN AVF cyclotron. *Nucl Instrum Meth Phys Res A* 425:409–414
  36. Weiss M (1973) Bunching of intense proton beams with six-dimensional matching to the LINAC acceptance. *IEEE Trans Nucl Sci* 20:877–879